

Prerequisites For DELTA-II Magnetic Measurements

Zachary Wolf
SLAC National Accelerator Laboratory

April 27, 2026

Abstract

The DELTA-II is an elliptically polarizing undulator that is being built at SLAC. After assembly, magnetic measurements are required to characterize the undulator. This note presents topics essential to the magnetic measurements including how to set the polarization modes and K value of the DELTA-II, the expected field profiles in the various polarization modes, and details of the magnetic measurement system.

1 Introduction¹

An elliptically polarizing undulator, DELTA-II, is being built at SLAC for use in the LCLS-II SXR line. The four quadrants of DELTA-II will be individually tuned and measured on a tuning bench. The four quadrants will then be assembled into the undulator. Magnetic measurements are required to characterize the assembled undulator. In order to do the magnetic measurements, several actions must be taken. One must set the magnet arrays to produce the various polarization modes, and one must set the undulator aperture to produce K parameter values in the operating range. The expected field configurations in the polarization modes must be understood. Finally, a setup for the measurements must be made which has the required accuracy to meet the undulator requirements. These and other subjects essential to the magnetic measurements are discussed in this note.

A previous DELTA undulator was built at SLAC for the original LCLS.² Many lessons were learned from the measurements of the original DELTA undulator, and the knowledge gained is being applied to the DELTA-II. Magnetic measurements of the original DELTA showed large phase errors. To avoid this problem, the DELTA-II will have much care put into the alignment of the magnet arrays since phase errors are sensitive to taper of the magnet arrays at the sub-10 μm level.³ The original DELTA had a transverse gradient in its K parameter.^{4,5,6} The DELTA-II's main distinguishing feature is the ability to move

¹Work supported in part by the DOE Contract DE-AC02-76SF00515. This work was performed in support of the LCLS project at SLAC.

²H.-D. Nuhn et al., "Commissioning Of The Delta Polarizing Undulator At LCLS", SLAC-PUB-16404, presented at the 37th International FEL Conference (FEL15), Daejeon, Korea.

³Z. Wolf, "Effect Of Quadrant Taper On Delta Undulator Phase Errors", LCLS-TN-15-2, February, 2015.

⁴Z. Wolf, "Position Dependence Of The K Parameter In The Delta Undulator", LCLS-TN-16-1, January, 2016.

⁵M. Calvi et al., "Transverse Gradient In Apple-Type Undulators", J. Synchrotron Rad (2017) 24, 600-608.

⁶H.-D. Nuhn, "Polarizing Afterburner For The LCLS-II Undulator Line", in *Proc. FEL2019*, Hamburg,

the quadrants radially in order to change the K value without introducing a gradient in K . Off-axis measurements of DELTA-II will be used to confirm a quadratic K dependence on transverse position without a linear term near the undulator axis. Measurements for the original DELTA were done with a Hall probe array involving an extensive set of calibrations.⁷ The DELTA-II measurements will be done with a single Hall probe which can be moved to different transverse positions. This will greatly simplify the Hall probe calibrations, and the method is more in line with the measurements of other undulators in the beam lines. With these and other refinements, we expect the DELTA-II undulator and its measurements will be an improvement compared to the original DELTA. We now proceed to discuss the DELTA-II undulator and its measurements.

2 General Information

2.1 Undulator Period

The period of the DELTA-II undulator is 49.33 mm. We wish to make the DELTA-II undulator resonant with the LCLS-II-HE undulators which have a period of 56.00 mm. The radiation wavelength of an undulator in the fundamental mode and in the forward direction is given by the resonance condition.

$$\lambda_r = \frac{\lambda_u}{2\gamma^2} \left(1 + \frac{1}{2} K^2 \right) \quad (1)$$

In this expression, λ_r is the radiation wavelength, λ_u is the undulator period, γ is the electron Lorentz factor, and $K^2 = K_x^2 + K_y^2$ is the undulator parameter accounting for slippage from electron motion in both directions transverse to the primary beam direction. For resonance, the DELTA-II undulator must radiate at the same wavelength as the HE-SXR undulators. This implies

$$\lambda_{u\Delta} \left(1 + \frac{1}{2} K_\Delta^2 \right) = \lambda_{uHE} \left(1 + \frac{1}{2} K_{HE}^2 \right) \quad (2)$$

where Δ refers to the DELTA-II undulator and HE refers to the HE-SXR undulators. To make the DELTA-II undulator resonant with the HE-SXR undulators, K_Δ must be

$$K_\Delta = \sqrt{2 \frac{\lambda_{uHE}}{\lambda_{u\Delta}} \left(1 + \frac{1}{2} K_{HE}^2 \right) - 2} \quad (3)$$

Similarly, if K_Δ is constrained by user requirements, the HE-SXR undulators must have

$$K_{HE} = \sqrt{2 \frac{\lambda_{u\Delta}}{\lambda_{uHE}} \left(1 + \frac{1}{2} K_\Delta^2 \right) - 2} \quad (4)$$

The K value of the DELTA-II undulator is required to vary in the operating range from $K_\Delta = 1.72$ to 7.35, as given in the requirements below. The HE-SXR undulators then must vary within the range $K_{HE} = 1.54$ to 6.89. These values are within the $1.51 \leq K_{HE} \leq 9.21$ operating range of the HE-SXR undulators.

Germany, Aug. 2019, paper WEP107, pp. 560-563. doi:10.18429/JACoW-FEL2019-WEP107

⁷Z. Wolf, "A Magnetic Measurement Plan For The Delta Undulator", LCLS-TN-13-4, March, 2013.

2.2 Coordinate System

The coordinate system for the DELTA-II undulator measurements is illustrated in figure 1. The coordinate system is right-handed with the z-axis in the beam direction, the y-axis is

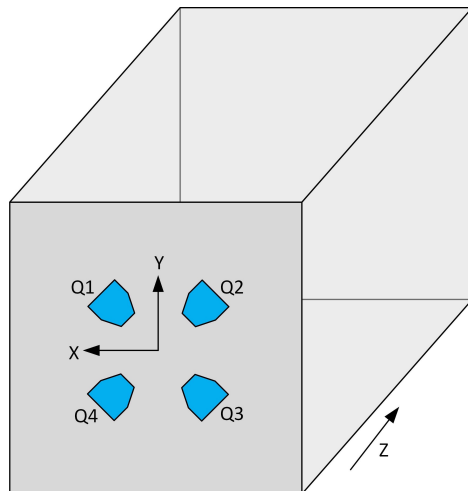


Figure 1: Coordinate system for the Delta-II measurements.

up, and the x-axis makes the system right-handed. Quadrant 1 has positive x and positive y. Quadrant 2 has negative x and positive y. Quadrant 3 has negative x and negative y. Quadrant 4 has positive x and negative y.

3 Undulator Mechanics

3.1 Polarization Control

Each quadrant of the DELTA-II has a magnet array in a Halbach configuration. The magnet array is held in a magnet carrier which is on a set of rails parallel to the beam axis that allows motion in the z-direction. This is illustrated in figure 2. The magnet array motion in the z-direction allows the polarization modes of the undulator to be set. The range of motion parallel to the z-direction is from -40 mm to $+40$ mm relative to the position where the rail ends are aligned. The required range of motion is one quarter an undulator period for setting the polarization modes, or $\Delta z = \pm \lambda_u / 4 = \pm (49.33 \text{ mm}) / 4 = \pm 12.3 \text{ mm}$, which is within the range of the rails.

3.2 K Value Control

The magnet array, magnet carrier, and the magnet carrier rails are mounted on a main carrier. The main carrier is also on a set of rails but these rails have a radially outward slope of 104.6 mrad relative to the $+z$ direction along the beam axis. Moving the main carrier on its rails in the $+z$ direction also moves the magnet array radially away from the beam axis. The radial motion is used to set the K value of the undulator. The range of

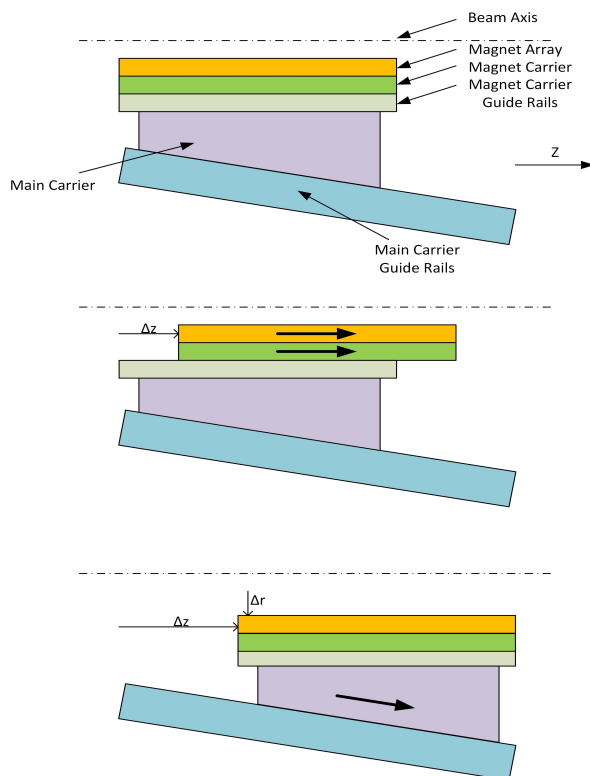


Figure 2: Each of the four quadrants can move in the z and radial directions.

motion along the angled rails is -40 mm to $+40$ mm relative to the position where the rail ends are aligned. The change in radial position when the main carrier is moved over its 80 mm range is $\Delta r = (80 \text{ mm}) \sin(0.1046) = 8.35$ mm. The beam pipe outer diameter is 6.00 mm, so its outer radius is 3.00 mm. With a 0.30 mm clearance from the magnets to the beam pipe, the minimum radial distance of the magnets to the beam axis is 3.30 mm. With the 8.35 mm range of radial motion, the magnet arrays can vary from 3.30 mm to 11.65 mm away from the beam axis. The diameter of the magnet aperture of the undulator then varies from 6.60 mm to 23.31 mm.

When a main carrier moves radially, it also moves longitudinally. The range of longitudinal motion is $\Delta z = (80 \text{ mm}) \cos(0.1046) = 79.6$ mm, or ± 39.8 mm relative to the position where the rail ends are aligned. This motion will affect the phase matching of the undulator. For a given undulator polarization mode, the magnetic measurements will determine the required phase integral for phase matching as a function of the undulator aperture. These phase matching results will include the effects of any longitudinal motion of the magnet arrays. For phase matching, the magnet arrays and main carriers must be set in the same way when the undulator is used as when the calibration is done.

A disadvantage of the longitudinal motion of the magnet arrays is that the source point of the undulator moves as the K value is changed. To eliminate the source point motion, the magnet arrays will be moved to compensate for the longitudinal motion of

the main carriers. This requires a motion of up to one quarter of an undulator period (for setting the polarization mode) plus the longitudinal motion of the main carrier: $\Delta z = \pm((49.33 \text{ mm})/4 + 39.8 \text{ mm}) = \pm 52.1 \text{ mm}$. This is beyond the $\pm 40 \text{ mm}$ limit of the magnet array rail motion. In these extreme cases, there must be shifts to the source point. The magnet arrays will be set using the required motion for polarization control plus a global longitudinal magnet array motion in the opposite direction to the main carrier longitudinal motion applied within the limits of the magnet array rail motion. At the extremes of the main carrier range, the source point will have small shifts.

3.3 Control System

Each quadrant has two motors, one motor for magnet array motion and one motor for main carrier motion. Both the magnet array and the main carrier in each quadrant have absolute encoders giving their position along their travel. In addition, the magnet arrays and main carriers have incremental encoders used for motion control. The incremental encoders can be used for position determination in case an absolute encoder fails. To use the incremental encoders for position determination, the position of each incremental encoder's index pulse must be determined.

In order to relate magnet array and main carrier positions to polarization modes and K values, an initial reference configuration must be established. The magnet array reference configuration has all four magnet arrays aligned so that the longitudinal magnetic center of each array is at the same z -position. The longitudinal magnetic center position of a magnet array is referenced to tooling balls during tuning. The tooling balls are used on a CMM to align the magnet arrays in the z -direction. In addition, the reference configuration is set when the rails for the magnet arrays are near their center position. Once the magnet arrays are in their reference configuration, the values of the absolute encoders must be recorded. Additionally, the incremental encoder position of each magnet array relative to the index pulse must be recorded.

The encoders on the magnet arrays give the magnet array z -position relative to the main carrier. We denote this by z_{qrel} where q is the quadrant number 1 to 4. We take the zero position of the magnet array relative to the main carrier to be the position in the reference configuration. In this case

$$z_{qrel} = s_q - s_{qref} \quad (5)$$

where s_q is the encoder reading for quadrant q , and s_{qref} is the encoder reading for quadrant q in the reference configuration. The radial position of the magnet array relative to the main carrier we take to be zero.

$$r_{qrel} = 0 \quad (6)$$

All radial position dependence comes from the main carriers.

The main carriers also have a reference configuration. The reference configuration is when the main carriers are positioned to give the minimum undulator bore aperture, determined as follows. First, the undulator mechanical axis is determined on a CMM from the geometry of the strongback. The magnetic axis and beam axis are made to coincide with the mechanical axis. We refer to the three common axes as the undulator axis. The minimum undulator bore mechanical aperture occurs when the magnets are 3.30

mm away from the undulator axis as discussed above under the section on K value control, however, magnetic effects must also be considered. During tuning, the magnet arrays are fiducialized to give all four arrays the same magnetic field strength at a position above the magnet array that is $\gtrsim 3.30$ mm. The tuning measurement axis is also aligned above the magnet array such that pitch and yaw in the magnetic field are removed. The measurement axis is fiducialized relative to the magnet array. On the CMM, the magnet array is placed so that the tuning measurement axis is on the undulator axis. The radial position of the main carriers when each tuning axis is on the undulator axis determines the reference configuration for the main carriers. When in the reference configuration, the value of each main carrier absolute encoder must be recorded. The position of each incremental encoder relative to its index pulse must be recorded.

The encoders on the main carriers give the position along the line angled relative to the undulator axis. We only consider identical moves of all four main carriers so that all four magnet arrays are always at the same radial position. We define the radial position of all four magnet arrays in the reference configuration to be 3.30 mm. The nominal value 3.30 mm can be used instead of the actual mechanical radius since the calibrations are done as a function of encoder reading, and for a given encoder reading, the undulator configuration will be the same when in use in the undulator hall as during the calibration in the MMF. Using the 3.30 mm value for the reference configuration, the radial position of all four magnet arrays is given by

$$r = 3.3 \text{ mm} + (s - s_{ref}) \sin(0.1046) \quad (7)$$

where s (without the subscript q) refers to the main carrier encoder reading, and s_{ref} refers to the main carrier encoder reading in the reference configuration. The factor $(s - s_{ref})$ is the same for all four main carriers.

The z-position of all four main carriers is given by

$$z_{carrier} = -39.8 \text{ mm} + (s - s_{ref}) \cos(0.1046) \quad (8)$$

Similar to the discussion above for the radial position, using the nominal value of -39.8 mm instead of a measured number leads to the same configuration when the undulator is operated as when it is calibrated.

Knowing the z-position of the main carriers, we can find the absolute z-positions of the magnet arrays. The z-positions of the magnet arrays are given by

$$z_q = z_{carrier} + z_{qrel} \quad (9)$$

$$= -39.8 \text{ mm} + (s - s_{ref}) \cos(0.1046) + (s_q - s_{qref}) \quad (10)$$

where z_q is the z-position of the magnet array for quadrant q .

The EPICS control system must have PVs which save the absolute encoder readings when the undulator is in the reference configuration. It must also have PVs which save each incremental encoder position relative to its index pulse when the undulator is in the reference configuration. The control system must also provide PVs for operating each of the eight motors, for reading the eight absolute encoders, and for reading the eight incremental encoders. PVs for temperature measurements are also required since the

magnet temperature during calibration must be recorded. During calibration, the undulator will sit on cam movers used to align the undulator to the measurement system. PVs to operate the cam movers must be provided.

In order to fully test the undulator plus its control system, additional PVs must be provided. PVs must be provided to set and read the gap (aperture) of the undulator. The PV to set the gap makes the four main carrier motors move the same radial distance away from the reference position. This involves calculating how far to move the main carriers given the angle of the rails relative to the undulator axis. The PV to read the gap similarly uses the main carrier absolute encoder positions and calculates the gap using the main carrier rail angles. Setting the undulator polarization modes must also have associated PVs. Setting the polarization mode involves moving each magnet array a fraction of the undulator period as defined in the section below. This means that PVs for the z-position of the magnet arrays relative to the carrier (z_{qrel}) must be provided. In addition, a global shift in the z-direction must be applied to all four magnet arrays in order to compensate for the longitudinal motion of the main carriers. A PV for the common z-position of all four carriers must be provided. Finally, PVs for the z-position of all four magnet arrays relative to the strongback (z_q) must be provided. A list of required PVs for magnetic measurements will be provided in the test plan.

Limit switches will be placed on each motor drive assembly so that no motion can exceed the limits of the drive. In addition, the Control Group's personnel must determine if the combined longitudinal motion of the magnet arrays and the main carriers can bring a magnet array in contact with an external device. If so, additional limit switches must be provided, possibly placed external to the undulator. Limit switches must be in place and tested before calibrations in the MMF can begin.

Setting the K value of the undulator in the undulator hall involves using the 'K as a function of gap' calibration done in the MMF plus corrections for the difference between the undulator temperature in the undulator hall and the undulator temperature during calibration. The temperature correction involves a parameter giving the change in magnet strength for a given change in temperature. The correction parameter for the other undulators was determined experimentally during a calibration in the MMF. A temperature calibration for the DELTA-II undulator will not be performed, and instead the nominal value for the magnet temperature coefficient from the magnet manufacturer will be used.

4 Fields In The Undulator

In this section we assume the radial position of each quadrant is fixed and is identical for all four quadrants. We consider the effect of moving the magnet arrays in the z-direction to set the polarization mode. After a general expression for the magnetic scalar potential is found, we calculate the magnetic fields in various polarization modes of the undulator.

Consider a single quadrant's magnet array on the tuning bench looking along the beam direction as shown in figure 3. We take the origin of the coordinate system in x and y on the magnetic axis of the assembled undulator. The origin in the z-direction is at the first

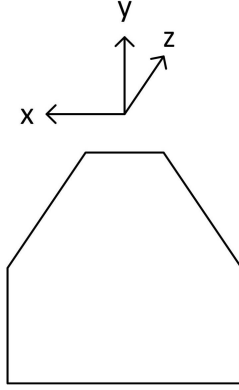


Figure 3: Coordinate system for a single quadrant's magnet array on the tuning bench.

peak field. The magnetic field above the magnet array obeys the following equations.

$$\nabla \times B = 0 \quad (11)$$

$$\nabla \cdot B = 0 \quad (12)$$

Since the curl of B is zero, B can be expressed in terms of a scalar potential, $B = -\nabla\phi$. The scalar potential obeys Laplace's equation.

$$\nabla^2\phi = 0 \quad (13)$$

To solve this equation, we use separation of variables.

$$\phi = X(x)Y(y)Z(z) \quad (14)$$

Laplace's equation becomes

$$\frac{X''}{X} + \frac{Y''}{Y} + \frac{Z''}{Z} = 0 \quad (15)$$

Since the sum of terms each containing a different independent variable is zero, each term must be a constant, and the sum of the constants must be zero.

$$\frac{X''}{X} = k_x^2 \quad (16)$$

$$\frac{Y''}{Y} = k_y^2 \quad (17)$$

$$\frac{Z''}{Z} = k_z^2 \quad (18)$$

$$k_x^2 + k_y^2 + k_z^2 = 0 \quad (19)$$

We only consider solutions periodic in z , so k_z is imaginary. We also know that the magnitude of the potential decreases as one moves away from the magnet array in the x -direction, and it is symmetric about $x = 0$. This means that the curvature of X is negative,

so k_x is imaginary. It also means that the gradient of X is zero near the beam axis so X does not contribute to the fields near the beam axis. We make an approximation that X is constant near the beam axis, but we keep the effect of the curvature of X by keeping k_x . Finally, we know that the magnitude of the potential decreases as one moves away from the magnet array in the y -direction. In the neighborhood of the beam axis, these conditions imply that the form of the potential is

$$\phi = \phi_0 \exp(-k_r y) \cos(k_u(z - z_0)) \quad (20)$$

where $k_u = 2\pi/\lambda_u$ where λ_u is the undulator period. Also, we use $k_r = k_y$ since it will involve the potential falloff in the radial direction of the assembled undulator. We take ϕ_0 positive so that the potential increases near a north pole and the field points away from a north pole. The term z_0 gives the z -position of the first north pole along the magnet array. The constraint from Laplace's equation becomes

$$k_r^2 = k_u^2 + |k_x|^2 \quad (21)$$

To find the potential in the assembled undulator, we take four copies of the potential from the tuning bench and rotate each one into its final orientation. This is illustrated for quadrant 1 in figure 4. To do the rotation, we first make the tuning bench coordinate

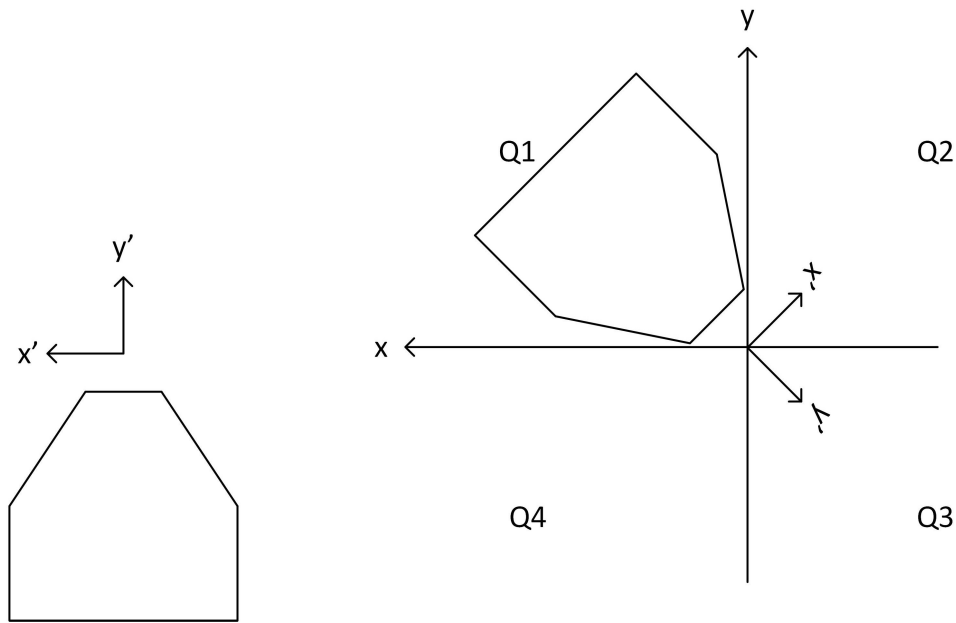


Figure 4: The assembled undulator is made by taking four magnet arrays from the tuning bench and rotating them into the final configuration. The rotation for quadrant 1 is shown.

system the ‘primed’ system and then apply a rotation matrix to get the coordinates in the assembled undulator system. When a quadrant is rotated about the beam axis by an angle θ from $+x$ toward $+y$, the x' , y' coordinates rotate with it. The x , y coordinates are fixed

and make a global system. The relation between the two sets of coordinates is

$$\begin{pmatrix} x \\ y \end{pmatrix} = \begin{pmatrix} \cos \theta & -\sin \theta \\ \sin \theta & \cos \theta \end{pmatrix} \begin{pmatrix} x' \\ y' \end{pmatrix} \quad (22)$$

The inverse relation is given by

$$\begin{pmatrix} x' \\ y' \end{pmatrix} = \begin{pmatrix} \cos \theta & \sin \theta \\ -\sin \theta & \cos \theta \end{pmatrix} \begin{pmatrix} x \\ y \end{pmatrix} \quad (23)$$

The scalar potential is invariant with respect to rotations as given by

$$\phi(x, y, z) = \phi(x', y', z') \quad (24)$$

where (x, y, z) and (x', y', z') refer to the same point. The scalar potential for a rotated quadrant is then given by

$$\phi(x, y, z) = \phi_0 \exp(-k_r(-x \sin \theta + y \cos \theta)) \cos(k_u(z - z_0)) \quad (25)$$

The rotation angle to go from the tuning bench orientation to the quadrant 1 orientation is $\theta = 135^\circ$. For quadrant 2, the rotation angle is $\theta = -135^\circ$. For quadrant 3, the rotation angle is $\theta = -45^\circ$. For quadrant 4, the rotation angle is $\theta = 45^\circ$. The magnets in quadrants 1 and 2 have opposite polarity from those in quadrants 3 and 4, so an extra minus sign must be added. The scalar potentials for the four quadrants are

$$\phi_1(x, y, z) = -\phi_0 \exp\left(-\frac{k_r}{\sqrt{2}}(-x - y)\right) \cos(k_u(z - z_{01})) \quad (26)$$

$$\phi_2(x, y, z) = -\phi_0 \exp\left(-\frac{k_r}{\sqrt{2}}(x - y)\right) \cos(k_u(z - z_{02})) \quad (27)$$

$$\phi_3(x, y, z) = \phi_0 \exp\left(-\frac{k_r}{\sqrt{2}}(x + y)\right) \cos(k_u(z - z_{03})) \quad (28)$$

$$\phi_4(x, y, z) = \phi_0 \exp\left(-\frac{k_r}{\sqrt{2}}(-x + y)\right) \cos(k_u(z - z_{04})) \quad (29)$$

In these expressions, z_{0i} is the position of the first pole in quadrant number i . It is noteworthy that quadrants 1 and 3 both have the same $(x + y)$ dependence, and quadrants 2 and 4 both depend on $(x - y)$. When adding the scalar potentials for the four quadrants to find the scalar potential for the assembled undulator, this leads us to group the scalar potentials for quadrants 1 and 3, and then group the scalar potentials for quadrants 2 and 4, and then add the terms to get the scalar potential for the whole undulator. The result can be interpreted as forming the entire undulator from two crossed undulators. A full calculation including setting the K value by shifting row 3 relative to row 1, and shifting row 4 relative to row 2, has been worked out.⁸ For DELTA-II, we do not need the shifts since we set K by changing the gap. For DELTA-II, $z_{01} = z_{03} := z_{013}$, and $z_{02} = z_{04} := z_{024}$. In this case, the scalar potential for the undulator is

$$\phi(x, y, z) = -2\phi_0 \sinh\left(\frac{k_r}{\sqrt{2}}(x + y)\right) \cos(k_u(z - z_{013})) \quad (30)$$

$$+2\phi_0 \sinh\left(\frac{k_r}{\sqrt{2}}(x - y)\right) \cos(k_u(z - z_{024})) \quad (31)$$

⁸Z. Wolf, "A Calculation Of The Fields In The Delta Undulator", LCLS-TN-14-1, January, 2014.

Using this potential, we now find the fields in various polarization modes.

4.1 Linear Polarization Vertical Magnetic Field (LPVMF)

Consider the linear polarization vertical magnetic field mode. The magnet sort was done so that this mode occurs when all the magnet arrays have $z_0 = 0$. The magnet arrays are illustrated in figure 5. The scalar potential in this case is

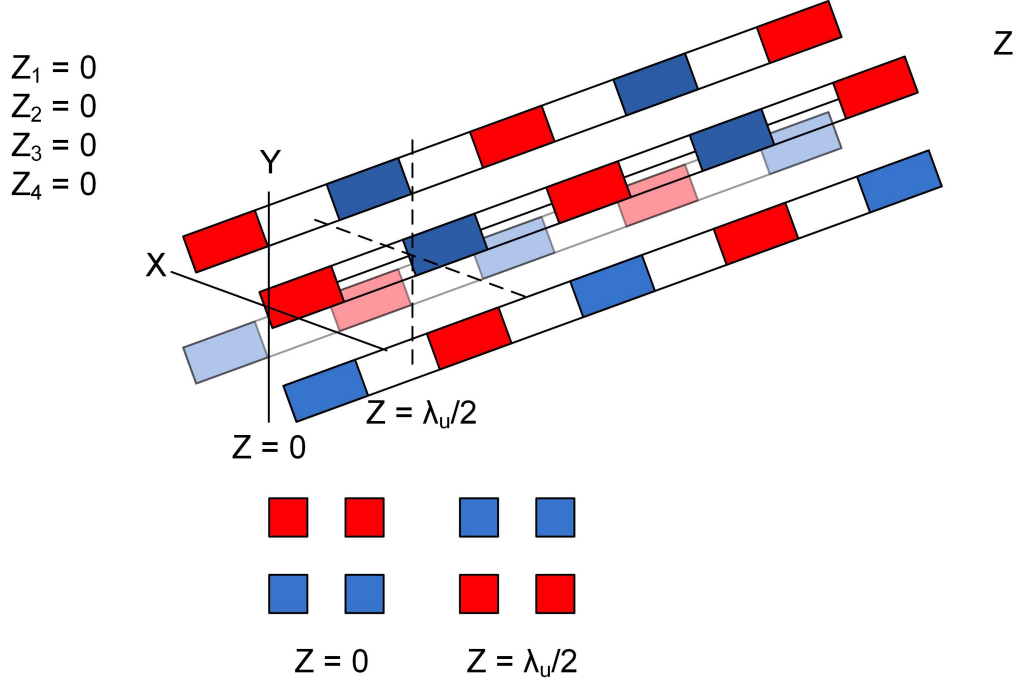


Figure 5: Linear polarization vertical magnetic field mode.

$$\begin{aligned}
 \phi(x, y, z) &= -2\phi_0 \sinh\left(\frac{k_r}{\sqrt{2}}(x+y)\right) \cos(k_u z) + 2\phi_0 \sinh\left(\frac{k_r}{\sqrt{2}}(x-y)\right) \cos(k_u z) \\
 &= -4\phi_0 \cosh\left(\frac{k_r}{\sqrt{2}}x\right) \sinh\left(\frac{k_r}{\sqrt{2}}y\right) \cos(k_u z)
 \end{aligned} \tag{32}$$

The fields $B = -\nabla\phi$ are

$$B_x = \frac{4\phi_0 k_r}{\sqrt{2}} \sinh\left(\frac{k_r}{\sqrt{2}}x\right) \sinh\left(\frac{k_r}{\sqrt{2}}y\right) \cos(k_u z) \tag{33}$$

$$B_y = \frac{4\phi_0 k_r}{\sqrt{2}} \cosh\left(\frac{k_r}{\sqrt{2}}x\right) \cosh\left(\frac{k_r}{\sqrt{2}}y\right) \cos(k_u z) \tag{34}$$

$$B_z = -4\phi_0 k_u \cosh\left(\frac{k_r}{\sqrt{2}}x\right) \sinh\left(\frac{k_r}{\sqrt{2}}y\right) \sin(k_u z) \tag{35}$$

On the undulator axis with $x = 0$, $y = 0$, the fields are

$$B_x = 0 \quad (36)$$

$$B_y = \frac{4\phi_0 k_r}{\sqrt{2}} \cos(k_u z) \quad (37)$$

$$B_z = 0 \quad (38)$$

4.2 Linear Polarization Horizontal Magnetic Field (LPHMF)

Now consider the linear polarization horizontal magnetic field mode of the undulator. This is shown in figure 6. Quadrants 1 and 3 have $z_{013} = 0$, and quadrants 2 and 4 have

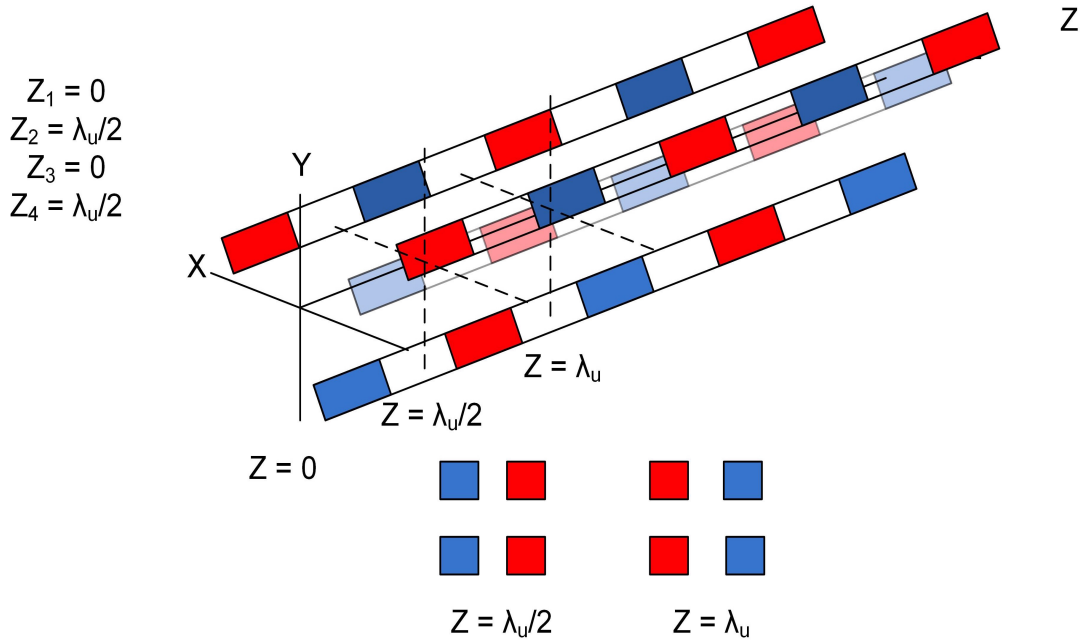


Figure 6: Linear polarization horizontal magnetic field mode.

$z_{024} = \lambda_u/2$. From equation 31, the scalar potential is

$$\begin{aligned} \phi(x, y, z) &= -2\phi_0 \sinh\left(\frac{k_r}{\sqrt{2}}(x+y)\right) \cos(k_u z) + 2\phi_0 \sinh\left(\frac{k_r}{\sqrt{2}}(x-y)\right) \cos(k_u z - \pi) \\ &= -4\phi_0 \sinh\left(\frac{k_r}{\sqrt{2}}x\right) \cosh\left(\frac{k_r}{\sqrt{2}}y\right) \cos(k_u z) \end{aligned} \quad (39)$$

The fields $B = -\nabla\phi$ are

$$B_x = \frac{4\phi_0 k_r}{\sqrt{2}} \cosh\left(\frac{k_r}{\sqrt{2}}x\right) \cosh\left(\frac{k_r}{\sqrt{2}}y\right) \cos(k_u z) \quad (40)$$

$$B_y = \frac{4\phi_0 k_r}{\sqrt{2}} \sinh\left(\frac{k_r}{\sqrt{2}}x\right) \sinh\left(\frac{k_r}{\sqrt{2}}y\right) \cos(k_u z) \quad (41)$$

$$B_z = -4\phi_0 k_u \sinh\left(\frac{k_r}{\sqrt{2}}x\right) \cosh\left(\frac{k_r}{\sqrt{2}}y\right) \sin(k_u z) \quad (42)$$

On the undulator axis with $x = 0$, $y = 0$, the fields are

$$B_x = \frac{4\phi_0 k_r}{\sqrt{2}} \cos(k_u z) \quad (43)$$

$$B_y = 0 \quad (44)$$

$$B_z = 0 \quad (45)$$

4.3 Circular Polarization Right Handed Magnetic Field (CPRMF)

Consider the undulator in circular polarization right handed magnetic field mode. The arrays are arranged as shown in figure 7. Quadrants 1 and 3 have $z_{013} = 0$, and quadrants

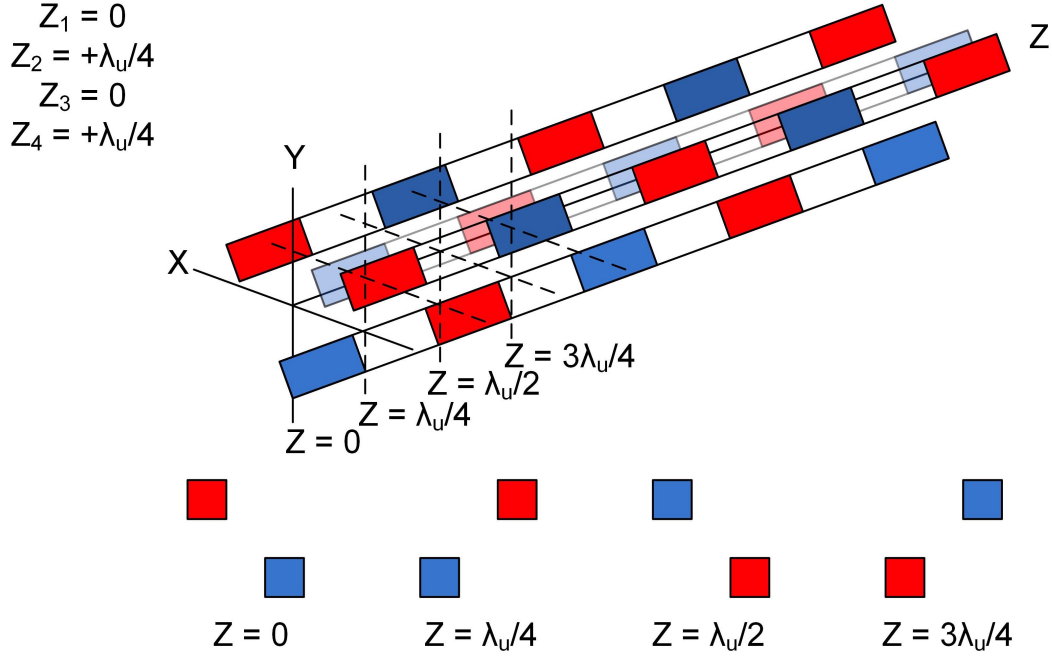


Figure 7: Circular polarization right hand magnetic field mode.

2 and 4 have $z_{024} = \lambda_u/4$. From equation 31, the scalar potential is

$$\begin{aligned}\phi(x, y, z) &= -2\phi_0 \sinh\left(\frac{k_r}{\sqrt{2}}(x+y)\right) \cos(k_u z) + 2\phi_0 \sinh\left(\frac{k_r}{\sqrt{2}}(x-y)\right) \cos\left(k_u z - \frac{\pi}{2}\right) \\ &= -2\phi_0 \sinh\left(\frac{k_r}{\sqrt{2}}(x+y)\right) \cos(k_u z) + 2\phi_0 \sinh\left(\frac{k_r}{\sqrt{2}}(x-y)\right) \sin(k_u z)\end{aligned}\quad (46)$$

The fields $B = -\nabla\phi$ are

$$\begin{aligned}B_x &= \frac{2\phi_0 k_r}{\sqrt{2}} \cosh\left(\frac{1}{\sqrt{2}}k_r(x+y)\right) \cos(k_u z) \\ &\quad - \frac{2\phi_0 k_r}{\sqrt{2}} \cosh\left(\frac{1}{\sqrt{2}}k_r(x-y)\right) \sin(k_u z)\end{aligned}\quad (47)$$

$$\begin{aligned}B_y &= \frac{2\phi_0 k_r}{\sqrt{2}} \cosh\left(\frac{1}{\sqrt{2}}k_r(x+y)\right) \cos(k_u z) \\ &\quad + \frac{2\phi_0 k_r}{\sqrt{2}} \cosh\left(\frac{1}{\sqrt{2}}k_r(x-y)\right) \sin(k_u z)\end{aligned}\quad (48)$$

$$\begin{aligned}B_z &= -2\phi_0 k_u \sinh\left(\frac{1}{\sqrt{2}}k_r(x+y)\right) \sin(k_u z) \\ &\quad - 2\phi_0 k_u \sinh\left(\frac{1}{\sqrt{2}}k_r(x-y)\right) \cos(k_u z)\end{aligned}\quad (49)$$

On the undulator axis with $x = 0$, $y = 0$, the fields are

$$B_x = \frac{2\phi_0 k_r}{\sqrt{2}} (\cos(k_u z) - \sin(k_u z))\quad (50)$$

$$B_y = \frac{2\phi_0 k_r}{\sqrt{2}} (\cos(k_u z) + \sin(k_u z))\quad (51)$$

$$B_z = 0\quad (52)$$

Simplifying, this becomes

$$B_x = 2\phi_0 k_r \cos\left(k_u z + \frac{\pi}{4}\right)\quad (53)$$

$$B_y = 2\phi_0 k_r \cos\left(k_u z - \frac{\pi}{4}\right)\quad (54)$$

$$B_z = 0\quad (55)$$

4.4 Circular Left Handed Polarization (CPLMF)

For circular polarization left handed magnetic field, the quadrants are arranged as shown in figure 8. Quadrants 1 and 3 have $z_{013} = \lambda_u/4$, and quadrants 2 and 4 have $z_{024} = 0$. From equation 31, the scalar potential is

$$\begin{aligned}\phi(x, y, z) &= -2\phi_0 \sinh\left(\frac{k_r}{\sqrt{2}}(x+y)\right) \cos\left(k_u z - \frac{\pi}{2}\right) + 2\phi_0 \sinh\left(\frac{k_r}{\sqrt{2}}(x-y)\right) \cos(k_u z) \\ &= -2\phi_0 \sinh\left(\frac{k_r}{\sqrt{2}}(x+y)\right) \sin(k_u z) + 2\phi_0 \sinh\left(\frac{k_r}{\sqrt{2}}(x-y)\right) \cos(k_u z)\end{aligned}\quad (56)$$

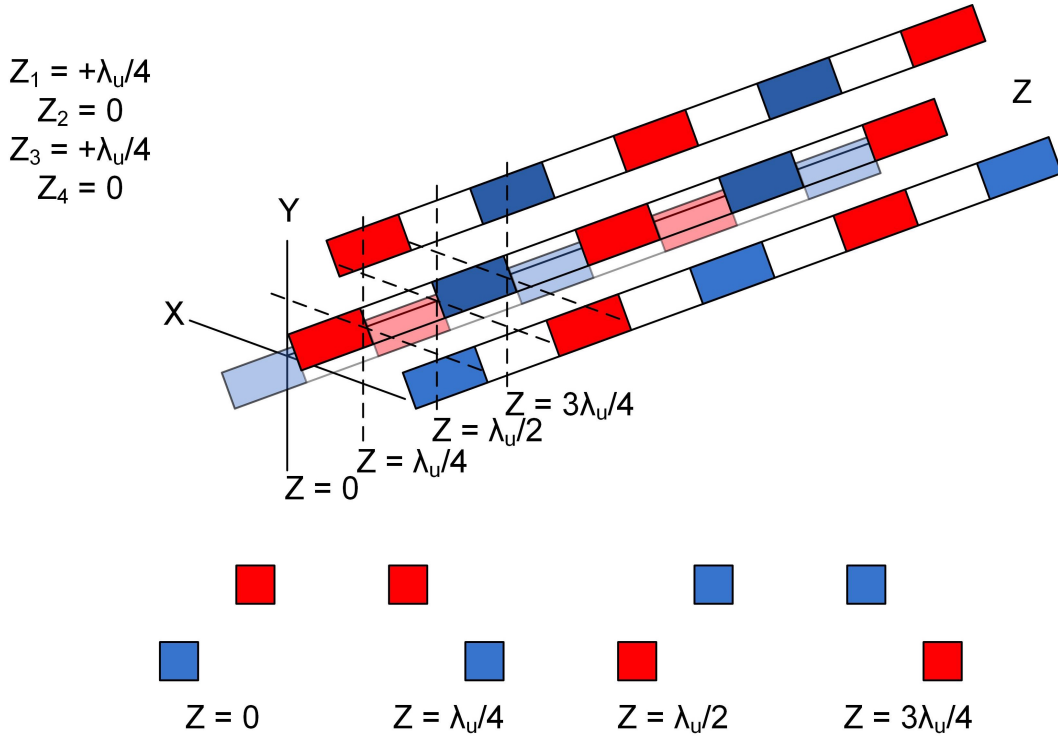


Figure 8: Circular polarization left hand magnetic field mode.

The fields $B = -\nabla\phi$ are

$$\begin{aligned}
 B_x &= \frac{2\phi_0 k_r}{\sqrt{2}} \cosh\left(\frac{1}{\sqrt{2}}k_r(x+y)\right) \sin(k_u z) \\
 &\quad - \frac{2\phi_0 k_r}{\sqrt{2}} \cosh\left(\frac{1}{\sqrt{2}}k_r(x-y)\right) \cos(k_u z)
 \end{aligned} \tag{57}$$

$$\begin{aligned}
 B_y &= \frac{2\phi_0 k_r}{\sqrt{2}} \cosh\left(\frac{1}{\sqrt{2}}k_r(x+y)\right) \sin(k_u z) \\
 &\quad + \frac{2\phi_0 k_r}{\sqrt{2}} \cosh\left(\frac{1}{\sqrt{2}}k_r(x-y)\right) \cos(k_u z)
 \end{aligned} \tag{58}$$

$$\begin{aligned}
 B_z &= 2\phi_0 k_u \sinh\left(\frac{1}{\sqrt{2}}k_r(x+y)\right) \cos(k_u z) \\
 &\quad + 2\phi_0 k_u \sinh\left(\frac{1}{\sqrt{2}}k_r(x-y)\right) \sin(k_u z)
 \end{aligned} \tag{59}$$

On the undulator axis with $x = 0$, $y = 0$, the fields are

$$B_x = \frac{2\phi_0 k_r}{\sqrt{2}} (\sin(k_u z) - \cos(k_u z)) \quad (60)$$

$$B_y = \frac{2\phi_0 k_r}{\sqrt{2}} (\sin(k_u z) + \cos(k_u z)) \quad (61)$$

$$B_z = 0 \quad (62)$$

Simplifying, this becomes

$$B_x = -2\phi_0 k_r \cos\left(k_u z + \frac{\pi}{4}\right) \quad (63)$$

$$B_y = 2\phi_0 k_r \cos\left(k_u z - \frac{\pi}{4}\right) \quad (64)$$

$$B_z = 0 \quad (65)$$

The CPLMF fields are the mirror reflection in the y-z plane of the CPRMF fields, as expected.

4.5 Elliptical Right Handed Polarization (EPRMF)

Repeating equation 31, the magnetic scalar potential in the undulator is

$$\begin{aligned} \phi(x, y, z) = & -2\phi_0 \sinh\left(\frac{k_r}{\sqrt{2}}(x+y)\right) \cos(k_u(z-z_{013})) \\ & + 2\phi_0 \sinh\left(\frac{k_r}{\sqrt{2}}(x-y)\right) \cos(k_u(z-z_{024})) \end{aligned} \quad (66)$$

Consider the case where $z_{013} = 0$ and $k_u z_{024} = \delta$. The scalar potential in this case is

$$\phi(x, y, z) = -2\phi_0 \sinh\left(\frac{k_r}{\sqrt{2}}(x+y)\right) \cos(k_u z) + 2\phi_0 \sinh\left(\frac{k_r}{\sqrt{2}}(x-y)\right) \cos(k_u z - \delta) \quad (67)$$

The fields $B = -\nabla\phi$ are

$$\begin{aligned} B_x = & \frac{2\phi_0 k_r}{\sqrt{2}} \cosh\left(\frac{1}{\sqrt{2}}k_r(x+y)\right) \cos(k_u z) \\ & - \frac{2\phi_0 k_r}{\sqrt{2}} \cosh\left(\frac{1}{\sqrt{2}}k_r(x-y)\right) \cos(k_u z - \delta) \end{aligned} \quad (68)$$

$$\begin{aligned} B_y = & \frac{2\phi_0 k_r}{\sqrt{2}} \cosh\left(\frac{1}{\sqrt{2}}k_r(x+y)\right) \cos(k_u z) \\ & + \frac{2\phi_0 k_r}{\sqrt{2}} \cosh\left(\frac{1}{\sqrt{2}}k_r(x-y)\right) \cos(k_u z - \delta) \end{aligned} \quad (69)$$

$$\begin{aligned} B_z = & -2\phi_0 k_u \sinh\left(\frac{1}{\sqrt{2}}k_r(x+y)\right) \sin(k_u z) \\ & + 2\phi_0 k_u \sinh\left(\frac{1}{\sqrt{2}}k_r(x-y)\right) \sin(k_u z - \delta) \end{aligned} \quad (70)$$

On the undulator axis with $x = 0$, $y = 0$, the fields are

$$B_x = \frac{2\phi_0 k_r}{\sqrt{2}} (\cos(k_u z) - \cos(k_u z - \delta)) \quad (71)$$

$$B_y = \frac{2\phi_0 k_r}{\sqrt{2}} (\cos(k_u z) + \cos(k_u z - \delta)) \quad (72)$$

$$B_z = 0 \quad (73)$$

Noting that

$$\begin{aligned} \cos(k_u z) - \cos(k_u z - \delta) &= \cos\left(k_u z - \frac{\delta}{2} + \frac{\delta}{2}\right) - \cos\left(k_u z - \frac{\delta}{2} - \frac{\delta}{2}\right) \\ &= -2 \sin\left(k_u z - \frac{\delta}{2}\right) \sin\left(\frac{\delta}{2}\right) \end{aligned} \quad (74)$$

and

$$\begin{aligned} \cos(k_u z) + \cos(k_u z - \delta) &= \cos\left(k_u z - \frac{\delta}{2} + \frac{\delta}{2}\right) + \cos\left(k_u z - \frac{\delta}{2} - \frac{\delta}{2}\right) \\ &= 2 \cos\left(k_u z - \frac{\delta}{2}\right) \cos\left(\frac{\delta}{2}\right) \end{aligned} \quad (75)$$

the equations for the fields simplify to

$$B_x = -\frac{4\phi_0 k_r}{\sqrt{2}} \sin\left(\frac{\delta}{2}\right) \sin\left(k_u z - \frac{\delta}{2}\right) \quad (76)$$

$$B_y = \frac{4\phi_0 k_r}{\sqrt{2}} \cos\left(\frac{\delta}{2}\right) \cos\left(k_u z - \frac{\delta}{2}\right) \quad (77)$$

$$B_z = 0 \quad (78)$$

As z increases, B_x and B_y trace out an ellipse.

$$\left(\frac{B_x}{\frac{4\phi_0 k_r}{\sqrt{2}} \sin\left(\frac{\delta}{2}\right)}\right)^2 + \left(\frac{B_y}{\frac{4\phi_0 k_r}{\sqrt{2}} \cos\left(\frac{\delta}{2}\right)}\right)^2 = 1 \quad (79)$$

Starting at $k_u z - \frac{\delta}{2} = 0$, B_y is a maximum and then decreases, B_x is zero and then goes negative, confirming that this is right handed polarization.

4.6 Elliptical Left Handed Polarization (EPLMF)

Starting again with equation 31, the magnetic scalar potential in the undulator is

$$\begin{aligned} \phi(x, y, z) &= -2\phi_0 \sinh\left(\frac{k_r}{\sqrt{2}}(x + y)\right) \cos(k_u(z - z_{013})) \\ &\quad + 2\phi_0 \sinh\left(\frac{k_r}{\sqrt{2}}(x - y)\right) \cos(k_u(z - z_{024})) \end{aligned} \quad (80)$$

Consider the case where $k_u z_{013} = \delta$ and $z_{024} = 0$. The scalar potential in this case is

$$\phi(x, y, z) = -2\phi_0 \sinh\left(\frac{k_r}{\sqrt{2}}(x+y)\right) \cos(k_u z - \delta) + 2\phi_0 \sinh\left(\frac{k_r}{\sqrt{2}}(x-y)\right) \cos(k_u z) \quad (81)$$

The fields $B = -\nabla\phi$ are

$$B_x = \frac{2\phi_0 k_r}{\sqrt{2}} \cosh\left(\frac{1}{\sqrt{2}}k_r(x+y)\right) \cos(k_u z - \delta) - \frac{2\phi_0 k_r}{\sqrt{2}} \cosh\left(\frac{1}{\sqrt{2}}k_r(x-y)\right) \cos(k_u z) \quad (82)$$

$$B_y = \frac{2\phi_0 k_r}{\sqrt{2}} \cosh\left(\frac{1}{\sqrt{2}}k_r(x+y)\right) \cos(k_u z - \delta) + \frac{2\phi_0 k_r}{\sqrt{2}} \cosh\left(\frac{1}{\sqrt{2}}k_r(x-y)\right) \cos(k_u z) \quad (83)$$

$$B_z = -2\phi_0 k_u \sinh\left(\frac{1}{\sqrt{2}}k_r(x+y)\right) \sin(k_u z - \delta) + 2\phi_0 k_u \sinh\left(\frac{1}{\sqrt{2}}k_r(x-y)\right) \sin(k_u z) \quad (84)$$

On the undulator axis with $x = 0$, $y = 0$, the fields are

$$B_x = \frac{2\phi_0 k_r}{\sqrt{2}} (\cos(k_u z - \delta) - \cos(k_u z)) \quad (85)$$

$$B_y = \frac{2\phi_0 k_r}{\sqrt{2}} (\cos(k_u z - \delta) + \cos(k_u z)) \quad (86)$$

$$B_z = 0 \quad (87)$$

Noting that

$$\begin{aligned} \cos(k_u z - \delta) - \cos(k_u z) &= \cos\left(k_u z - \frac{\delta}{2} - \frac{\delta}{2}\right) - \cos\left(k_u z - \frac{\delta}{2} + \frac{\delta}{2}\right) \\ &= 2 \sin\left(k_u z - \frac{\delta}{2}\right) \sin\left(\frac{\delta}{2}\right) \end{aligned} \quad (88)$$

and

$$\begin{aligned} \cos(k_u z - \delta) + \cos(k_u z) &= \cos\left(k_u z - \frac{\delta}{2} - \frac{\delta}{2}\right) + \cos\left(k_u z - \frac{\delta}{2} + \frac{\delta}{2}\right) \\ &= 2 \cos\left(k_u z - \frac{\delta}{2}\right) \cos\left(\frac{\delta}{2}\right) \end{aligned} \quad (89)$$

the equations for the fields simplify to

$$B_x = \frac{4\phi_0 k_r}{\sqrt{2}} \sin\left(\frac{\delta}{2}\right) \sin\left(k_u z - \frac{\delta}{2}\right) \quad (90)$$

$$B_y = \frac{4\phi_0 k_r}{\sqrt{2}} \cos\left(\frac{\delta}{2}\right) \cos\left(k_u z - \frac{\delta}{2}\right) \quad (91)$$

$$B_z = 0 \quad (92)$$

As z increases, B_x and B_y trace out an ellipse.

$$\left(\frac{B_x}{\frac{4\phi_0 k_r}{\sqrt{2}} \sin\left(\frac{\delta}{2}\right)}\right)^2 + \left(\frac{B_y}{\frac{4\phi_0 k_r}{\sqrt{2}} \cos\left(\frac{\delta}{2}\right)}\right)^2 = 1 \quad (93)$$

Starting at $k_u z - \frac{\delta}{2} = 0$, B_y is a maximum and then decreases, B_x is zero and then goes positive, confirming that this is left handed polarization.

4.7 Magnet Array Position Settings

In each case above when calculating the fields, the magnet arrays were moved toward $+z$. This motion shifts the source point in the different modes. To correct this, we can perform global shifts to all four quadrants without changing the magnetic fields. We now apply global shifts to center the average position of the magnet arrays on the main carriers. This defines our baseline quadrant row setting for the polarization modes.

We start with positive shifts of $z = 0, \lambda_u/8, \lambda_u/4, 3\lambda_u/8, \lambda_u/2$ for linear, elliptical, and circular modes. By shifting z_{013} or z_{024} we get left handed or right handed polarization. By applying global shifts so the undulator center remains at $z = 0$, we get the baseline quadrant row settings given in the following table.

| Mode | Z01 | Z02 | Z03 | Z04 |
|-------|------------------|------------------|------------------|------------------|
| LPVMF | 0 | 0 | 0 | 0 |
| EPRM1 | $-\lambda_u/16$ | $\lambda_u/16$ | $-\lambda_u/16$ | $\lambda_u/16$ |
| EPLM1 | $\lambda_u/16$ | $-\lambda_u/16$ | $\lambda_u/16$ | $-\lambda_u/16$ |
| CPRMF | $-\lambda_u/8$ | $\lambda_u/8$ | $-\lambda_u/8$ | $\lambda_u/8$ |
| CPLMF | $\lambda_u/8$ | $-\lambda_u/8$ | $\lambda_u/8$ | $-\lambda_u/8$ |
| EPRM2 | $-3\lambda_u/16$ | $3\lambda_u/16$ | $-3\lambda_u/16$ | $3\lambda_u/16$ |
| EPLM2 | $3\lambda_u/16$ | $-3\lambda_u/16$ | $3\lambda_u/16$ | $-3\lambda_u/16$ |
| LPHMF | $-\lambda_u/4$ | $\lambda_u/4$ | $-\lambda_u/4$ | $\lambda_u/4$ |

Table 1: Magnet array positions for each polarization mode.

A plot of B_y vs B_x as z varies over an undulator period in EPRMF mode is shown in figure 9. Using the notation given above for the right hand elliptical polarization calculation $\delta = k_u z_{024}$, the figure shows plots for values of $\delta = [0 \text{ to } 8] * \lambda_u/8$. The fields are normalized to $B_0 = \frac{4\phi_0 k_r}{\sqrt{2}}$.

We will also add additional global shifts to the magnet arrays to compensate for the longitudinal main carrier motion. When setting the K value, if the longitudinal shift of the main carriers is $\Delta z = \Delta s \cos(0.1046)$, where Δs is the distance moved along the rails, we will add the negative of this to all four magnet array positions to compensate for the longitudinal main carrier motion. At the limits of the K range, the compensation for main carrier motion will exceed the range of the magnet array rails. In this case only motion within the limits of the magnet array rails will be applied and small motions of the undulator source point at the limits of the main carrier motion will result.

In the original DELTA undulator, the K value was set by shifting the magnet arrays in a configuration equivalent to two crossed adjustable phase undulators. There were four

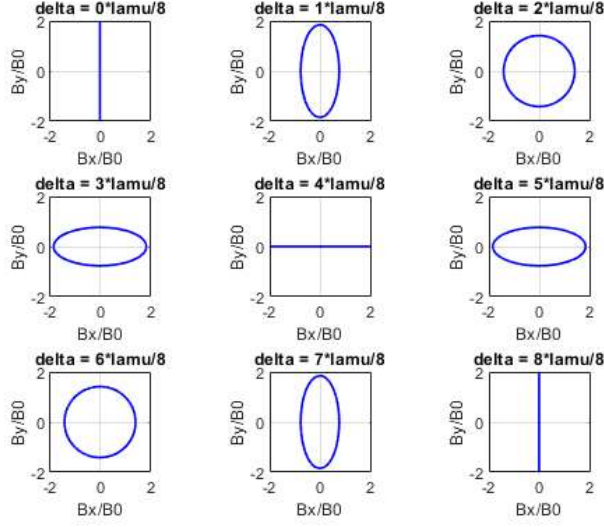


Figure 9: B_y vs B_x as z varies over an undulator period for various values of δ .

ways to make these shifts, making four "kinds" of settings. For DELTA-II, the K value is set by moving the magnet arrays radially. The "kind" settings of the original DELTA are not necessary.

4.8 Alignment Considerations

The fields in the undulator dictate how accurately the beam needs to be placed on the magnetic axis. In typical modes the field varies as $\cosh\left(\frac{k_r}{\sqrt{2}}x\right)$ or $\cosh\left(\frac{k_r}{\sqrt{2}}y\right)$. We estimate that $|k_x| \simeq k_u$ in the relation $k_r^2 = k_u^2 + |k_x|^2$, so the value of $k_r \simeq \sqrt{2}k_u$. In this case the fields vary approximately as $\cosh(k_u x)$ or $\cosh(k_u y)$ as in a planar undulator. The value of k_u is $k_u = \frac{2\pi}{\lambda_u} = 0.127$ 1/mm. The value of $\cosh(k_u y)$ changes by 1×10^{-4} when $k_u y = 0.0141$. If we want to keep B_y , and therefore K , within the range of 1×10^{-4} of its measured value, we need the beam to be within 0.111 mm of the magnetic axis. Since we don't want to use all of our K tolerance on alignment errors, we take a value of 100 μm as the combined fiducialization plus alignment error budget.

The Hall probe is guided by a beam pipe used only for measurements and which is installed in the lower half of the undulator. The beam pipe is straightened and measured on a CMM. We wish to measure on a straight line along the magnetic axis. Transverse position deviations of up to 100 μm can be tolerated while keeping the Hall probe measurements at a given z -position accurate to one part in 10^4 .

5 Magnetic Measurements Setup

The DELTA-II undulator will be measured in the assembly area of the MMF. An overview of the measurement setup is shown in figure 10. The undulator is placed on pedestals with cam

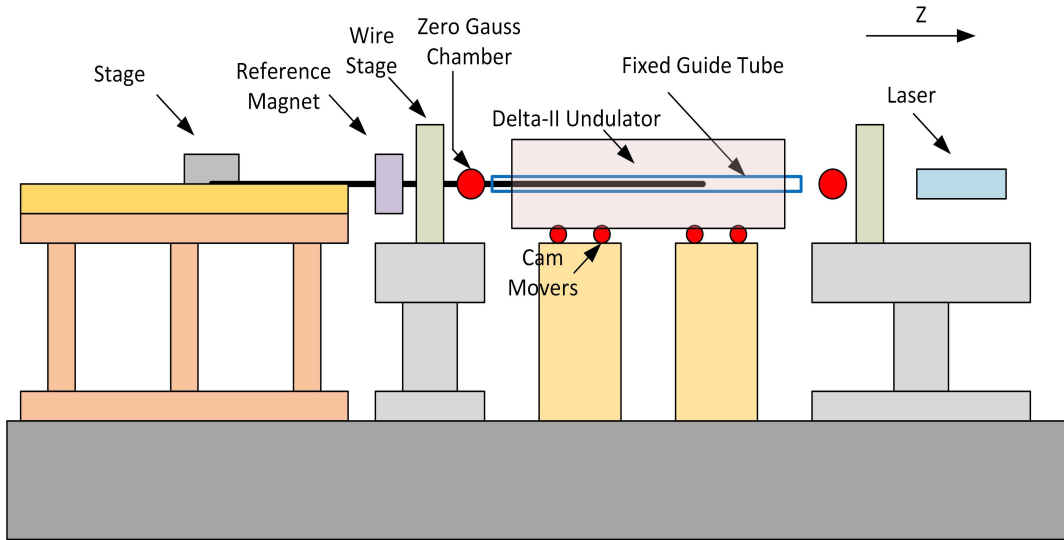


Figure 10: An overview of the magnetic measurement setup for the Delta-II measurements.

mover adjustments. Stands are placed on both ends of the undulator to hold measurement equipment. A stretched wire system is used to measure magnetic field integrals. Zero Gauss chambers are placed before and after the undulator and are used to take out offsets when doing Hall probe measurements. Fiducialization magnets will be placed on the pedestals when the position of the Hall probe must be determined. A reference magnet is used to align the Hall probe's roll angle. The Hall probe is moved through the undulator using a long stage. The beam pipe in the undulator is made straight on a CMM and is used to guide the Hall probe's transverse position. After measurements, the beam pipe used for the measurements will be replaced with a new polished beam pipe suitable for operation with the electron beam.

The components on the pedestal at the upstream end of the undulator are shown in figure 11. The zero Gauss chamber is placed closest to the undulator, but care must be taken so that the undulator magnets do not get so close that they magnetize the chamber. The zero Gauss chamber must be located at least 20 cm away from the magnet arrays when they are located as far upstream as possible. This will occur when the magnet arrays are moved upstream by 40 mm and the main carriers are also moved upstream by 40 mm. The zero Gauss chamber must then be $20\text{ cm} + 4\text{ cm} + 4\text{ cm} = 28\text{ cm}$ away from the strongback of the undulator. The zero Gauss chamber will be replaced by a fiducialization magnet when the Hall probe position must be determined. The fiducialization magnet must be absent during magnetic measurements, but must be near the undulator when in use so that straightness errors in the beam pipe will have minimal effect. The beam pipe used for measuring the DELTA-II undulator must extend past the undulator and through the

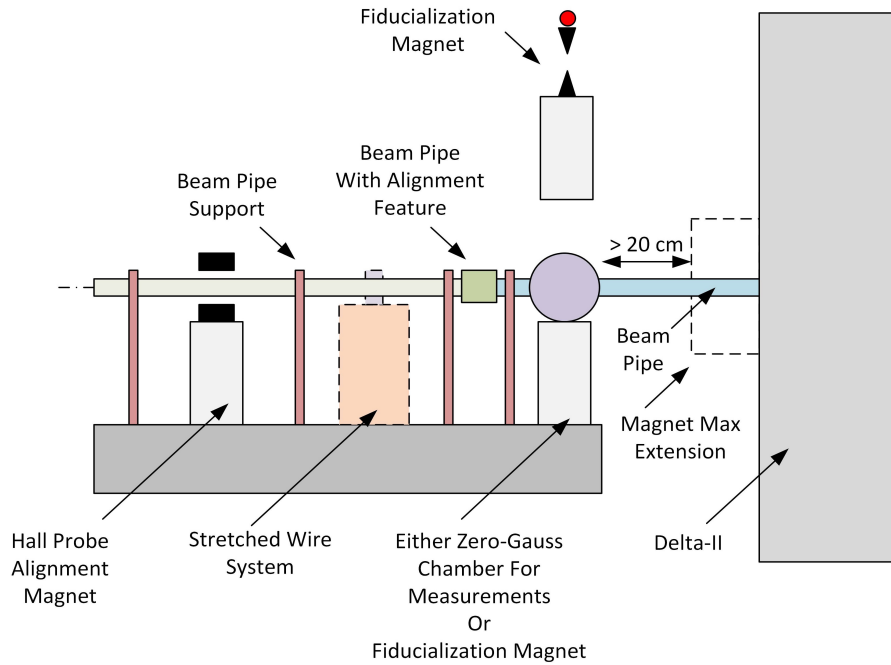


Figure 11: Components on the pedestal at the upstream end of the undulator.

zero Gauss chamber to a support stand. Allowing 20 cm for the zero Gauss chamber and support stand, the beam pipe must extend 48 cm past the strongback of the undulator. At the end of the beam pipe through the undulator, an auxiliary beam pipe section must be joined to allow inserting the Hall probe into the undulator beam pipe. This auxiliary beam pipe section must have a feature such as a ferrule which aligns the beam pipes so that the Hall probe can pass smoothly across the junction. The auxiliary beam pipe must also have support stands. The auxiliary beam pipe allows the Hall probe to move to the alignment magnet. For stretched wire measurements, the auxiliary beam pipe must be pulled back to allow the stages for the measurement to be inserted. Additionally, the auxiliary beam pipe must be pulled back to allow different positioning feet on the Hall probe package to be inserted which position the Hall probe transversely in the beam pipe. The configuration for replacing the positioning feet on the Hall probe package is shown in figure 12. A fiducialization magnet can be placed in the space previously occupied by the stretched wire stage in order to check that the Hall probe moved according to the positioning feet that were added to the Hall probe package.

The pedestal at the downstream end of the undulator also has provisions for a zero Gauss chamber, a fiducialization magnet, and a stretched wire stage. The downstream end pedestal is shown in figure 13. The beam pipe must extend 48 cm past the end of the undulator strongback, the same as at the entrance end. A support holds the extended beam pipe. The functions of the zero Gauss chamber, the fiducialization magnets, and the stretched wire stage are the same as for the components on the entrance end pedestal. In addition, an optical system is placed on the downstream end pedestal. The optical system

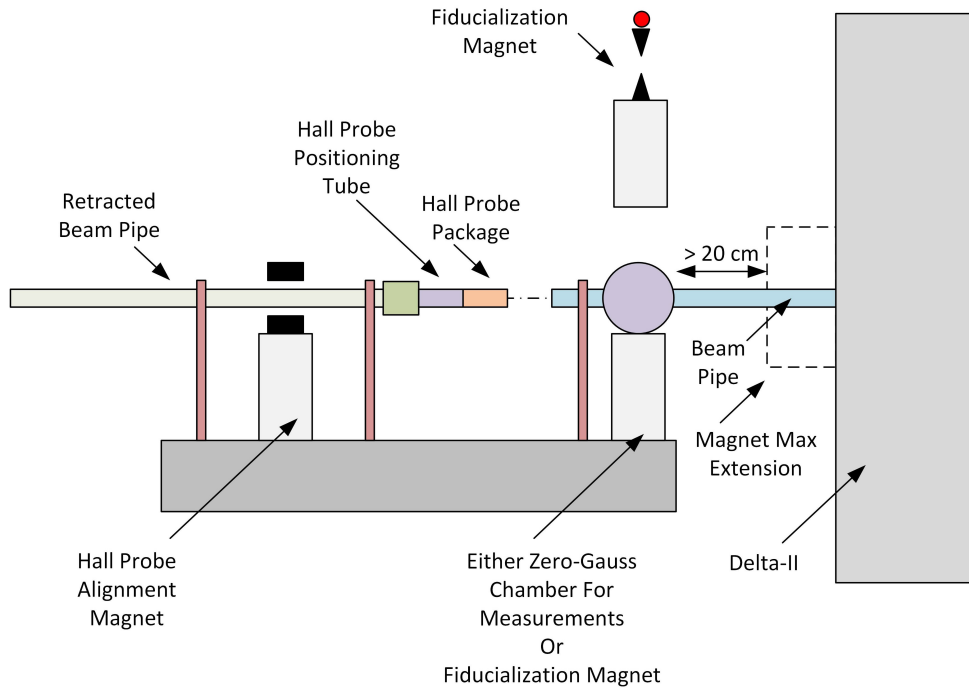


Figure 12: The second beam pipe is retracted to allow replacing the positioning feet on the Hall probe package.

gives the Hall probe z-position by interferometry. The Hall probe system generates triggers for the measurements, and for each trigger, the interferometer reading is written to a file. The file is used in the analysis to give the z-position of each Hall probe measurement. The x and y positions of the Hall probe are also obtained from the optical system by using a camera to locate the reflected beam from a corner cube on the Hall probe holder. The x and y position determination is illustrated in figure 14.

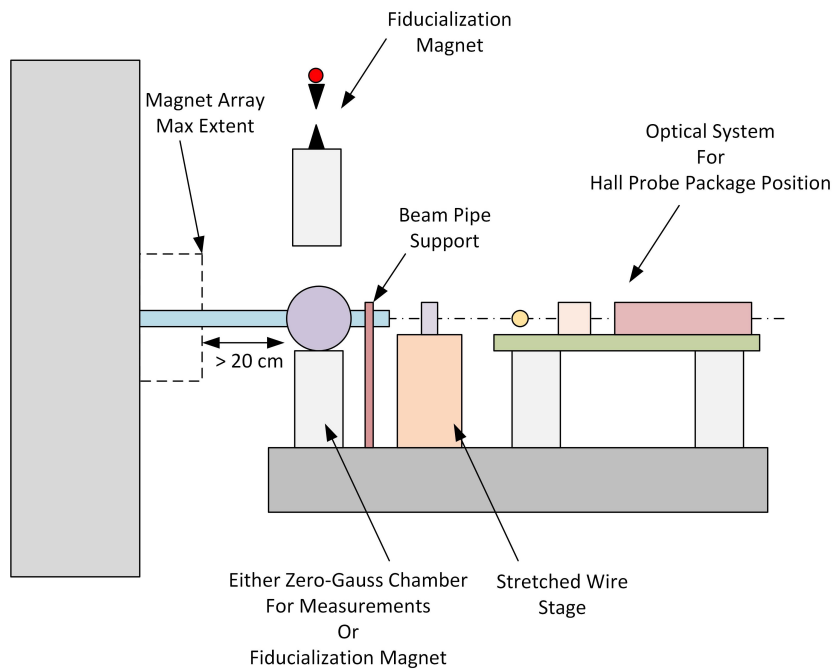


Figure 13: Pedestal components on the downstream end of the undulator.

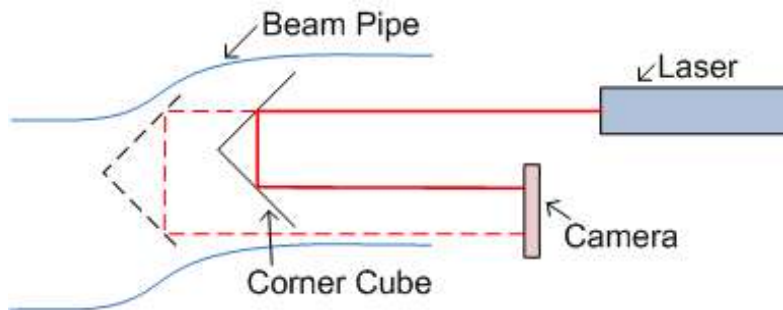


Figure 14: A corner cube is used to find the transverse location of the probe.

6 Conclusion

This note presented information required to make the DELTA-II magnetic measurements. Details for setting the magnet arrays to produce various polarization modes and various K values were presented. Calculations of the expected fields in the undulator were made. The setup for the magnetic measurements was presented. This note is a companion to the detailed test plan for the measurements.

Acknowledgements

Many thanks to Yurii Levashov, Johann Baader, and Heinz-Dieter Nuhn for valuable discussions.